PROCEEDINGS OF SCIENCE

# Indirect study of $^{60}$Fe(n,$\gamma$)$^{61}$Fe via the transfer reaction d($^{60}$Fe,p$\gamma$) $^{61}$Fe

**S. Giron*** [a], **F. Hammache** [a], **N. de Séréville** [a], **D. Beaumel** [a], **J. Burgunder** [b], **L. Caceres** [b], **G. Duchêne** [c], **E. Clement** [b], **B. Fernandez** [b], **F. Flavigny** [d], **G. De France** [b], **S. Franchoo** [a], **D. Galaviz-Redondo** [e], **L. Gasques** [e], **J. Gibelin** [f], **A. Gillibert** [d], **S. Grevy** [b], **J. Guillot** [a], **M. Heil** [g], **J. Kiener** [h], **V. Lapoux**[d], **F. Maréchal** [a], **A. Matta** [a], **I. Matea** [a], **M. Moukaddam** [c], **L. Nalpas** [d], **L. Perrot** [a], **A. Obertelli** [d], **R. Raabe** [b], **P. Roussel** [a], **J. A. Scarpaci** [a], **O. Sorlin** [b], **I. Stefan** [a], **C. Stoedel** [b], **M. Takechi** [i], **J. C. Thomas** [b], **Y. Togano** [i]

[a] *Institut de Physique Nucléaire, UMR8608, CNRS/IN2P3 and Université Paris-Sud XI, F-91406 Orsay, France*
[b] *GANIL,CEA/DSM-CNRS/IN2P3, Bd Henri Becquerel, BP 55027, F-14076 Caen Cedex 5, France*
[c] *IPHC-DRS, UdS, IN2P3-CNRS 23 rue du Loess, BP 28, 67037 Strasbourg, Cedex 2, France*
[d] *CEA-Saclay, DSM/IRFU/SPhN, F-91191 Gif sur Yvette Cedex, France*
[e] *Centro de Fisica Nuclear da Universidade de Lisboa, 1649-003, Lisboa, Portugal*
[f] *LPC Caen (IN2P3-CNRS/ISMRA et Université, F-14050, Caen Cedex, France*
[g] *GSI Helmholtzzentrum fur Schwerionenforschung GmbH, D-64291 Darmstadt, Germany*
[h] *CSNSM, UMR 8609, CNRS/IN2P3 and Université Paris Sud 11, F-91405 Orsay, France*
[i] *RIKEN Nishina Center, 2-1 Hirosawa, Wako, Saitama 351-0198, Japan*
*E-mail:* giron@ipno.in2p3.fr

$^{60}$Fe nuclei play an important role both in $\gamma$-ray astronomy and in pre-solar grains study. The interpretation of these observations depends on a reliable $^{60}$Fe yield prediction. We report here on the d($^{60}$Fe,p$\gamma$)$^{61}$Fe experiment performed at GANIL, aiming at studying the $^{60}$Fe(n,$\gamma$)$^{61}$Fe reaction to reduce nuclear uncertainties surrounding $^{60}$Fe nucleosynthesis. Preliminary results concerning excitation energies of $^{61}$Fe are presented.

*11th Symposium on Nuclei in the Cosmos, NIC XI*
*July 19-23, 2010*
*Heidelberg, Germany*

*Speaker.

 

PoS(NIC XI)190

## 1. Introduction

$^{60}$Fe plays an important role in different contexts in astrophysics. Caracteristic $\gamma$-ray lines issued from the radioactive decay chain $^{60}$Fe- $^{60}$Co- $^{60}$Ni were recently detected by INTEGRAL [1] and RHESSI [2] spacecrafts which confirm, since $^{60}$Fe lifetime ($T_{1/2} = 2.62 \pm 0.004$Myr [3]) is short compared with the time scale of the chemical evolution of the Galaxy ($\approx 10^{10}$yr), that $^{60}$Fe nucleosynthesis is still active. $^{60}$Fe is also observed in pre-solar grains after its decay in $^{60}$Ni [4] which is relevant to understand the conditions of formation of the early solar system. Last, observations of $^{60}$Fe in sediments of the deep ocean crust have been related to the explosion of a supernova in the vicinity of the Earth, million years ago [5]. The interpretation of all these observations depends on reliable $^{60}$Fe yields prediction.

$^{60}$Fe is believed to be mainly produced in core-collapse supernovae [6] during explosive O-Ne burning and in the He-burning shell by successive neutron captures on Fe-peak nuclei (s-process). In a lesser extent, it is also produced in AGB [7] and Wolf-Rayet stars. Stellar models include several inputs such as convection, mass loss or reaction rates, which should all be controlled to calculate reliable yields. In particular, the cross-sections of $^{59}$Fe(n,$\gamma$)$^{60}$Fe and $^{60}$Fe(n,$\gamma$)$^{61}$Fe reactions, involved in $^{60}$Fe nucleosynthesis, suffer from large uncertainties. Until recently [8], reaction rates were based on Hauser-Feshbach calculations, no experimental data being available for those reactions.

Reaction rates of radiative capture have two components: a resonant component involving levels above neutron threshold, and a direct contribution involving levels below neutron threshold. In the case of $^{60}$Fe(n,$\gamma$)$^{61}$Fe the direct component is likely not to be negligible compared with the resonant capture part, due to a relatively small value of the neutron threshold ($S_n = 5.58$ MeV). Hence, using (d,p) neutron transfer reaction for this case can help to improve the knowledge of $^{61}$Fe spectroscopy [9] [10] (excitation energy, spin-parity and spectroscopic factors) which is important both to determine the direct component of the cross-section, and to constrain shell model calculations used in Hauser-Feshbach calculations.

Accordingly, a d($^{60}$Fe,p$\gamma$)$^{61}$Fe experiment was recently performed at GANIL to measure the excitation energy of the different populated levels of $^{61}$Fe as well as their proton angular distributions. The corresponding spectroscopic factors and angular momentum will be extracted respectively from normalization and comparison of the shape of the experimental proton angular distributions with theoretical distributions based on DWBA calculations.

## 2. Experimental setup

The $^{60}$Fe secondary beam was produced by fragmentation of a $^{64}$Ni beam (accelerated up to 55 A.MeV by the cyclotrons of GANIL) on a 500$\mu$m $^{9}$Be target placed at the entrance of the LISE spectrometer [11]. The $^{60}$Fe beam was then selected in mass and charge by two magnetic dipoles and in velocity by a Wien filter. After passing through a 700$\mu$m thick degrader, a $^{60}$Fe beam of 27 MeV/u with $10^5$ pps intensity and 70% purity was obtained and sent on a 2mg/cm$^2$ $CD_2$ target.

The experimental setup (see Fig.1) was composed of charged particles and $\gamma$-ray detectors, as well as an ionization chamber and a plastic placed downstream the target, allowing an identification in charge of the heavy fragments via time of flight and energy measurement.

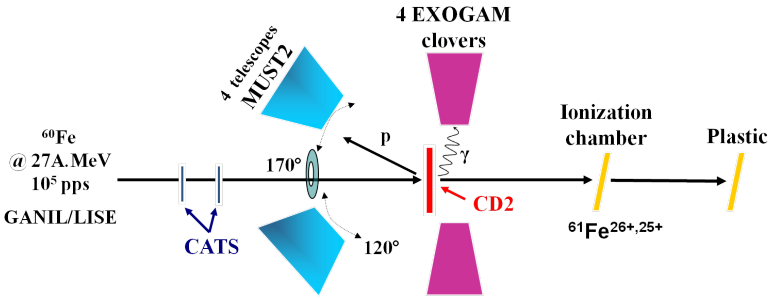


Figure 1: *Scheme of the experimental setup.*

Two beam tracking detectors CATS [12], were placed in the beam 95.6 and 45.6 cm upstream the target. These multiwire proportionnal chambers with a $70 \times 70$ cm$^2$ active area allow to reconstruct the position of incident ions event by event using charges deposited on several strips of the cathode [13] with a good resolution ($\lesssim 0.1$ mm) leading to a position resolution of the beam impact on target of $\sim 1$ mm. Indeed, $^{60}$Fe being produced by fragmentation, the beam emittance and the beam spot on target are large (1 cm in X, 2 mm in Y). A precise reconstruction of the beam impact on target is thus required to determine accurately the proton emission point and angle.

Protons were detected at backward angles by an annular Double-sided Silicon Strip Detector (DSSD) and 4 MUST2 telescopes [14], made of three stages. The first one is a DSSD of $10\times10$ cm$^2$ area and 300 $\mu$m thickness. It is made of 128 strips in X and Y and used for position (strip pitch: 0.7 mm) and energy loss measurement (35 keV FWHM resolution with a 3-$\alpha$ source). The second stage is composed of 16 pads of Si(Li) of 5 mm thickness and $2.5\times2.5$ cm$^2$ area ($\sim 80$ keV FWHM energy resolution) for energy residual measurement. The last one, consisting in 16 CsI crystals (4 cm thick) designed for energy measurement, was not used for this experiment. The silicon annular detector, designed by Micron as S1, is 500 $\mu$m thick and is composed of 64 strips of 1.4 mm and 16 wedges for position localization and energy measurement ($\sim 50$ keV resolution with a 3-$\alpha$ source). For the ground state, the angular coverage at backward angles of MUST2 telescopes and the annular detector is 2.51 -22.77° in the CM frame (121-172° in the laboratory frame).

The expected resolution on excitation energy ($\sim 700$ keV) will be improved by the use of four EXOGAM clovers ($\sim$3 keV resolution for the $\gamma$-ray at 1.3 MeV of $^{60}$Co) placed close to the target ($\sim 5$ cm) to detect $\gamma$-rays in coincidence.

## 3. Experimental results

Proton emission angle was reconstructed using the beam interaction position on target and the direction of the beam reconstructed from CATS detectors, as well as the position of the detected protons in MUST2 DSSD layer. The angular precision on the proton emission angle is $\sim 2.2°$ in the laboratory frame.

Depending on the charged particles energy, particles stop or punch through the DSSD layer. When they stop in the DSSD layer, the identification is performed via Time of Flight technique (see Fig.2 left), whereas particles that punch through the DSSD layer and stop in the Si(Li) detector are

identified via ΔE technique (see Fig.2 right). In both cases, a clear identification of protons is achieved.

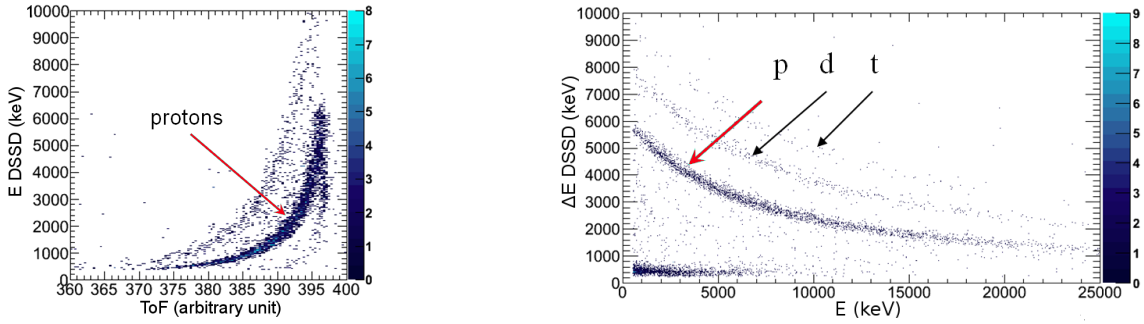


Figure 2: *Proton identification in MUST2 telescopes. Left: Energy versus Time of Flight (ToF) selection, where ToF is measured with respect to CATS detector; data of 2 telescopes are summed. Right: ΔE-E selection, where ΔE is the energy loss of particles in the first layer of MUST2 detectors, and E the energy deposit of particles in the Si(Li) detector; data of 3 telescopes are summed.*

Kinematic lines (total energy versus angle) were extracted from proton emission angle calculated from MUST2 position and the energy deposit in DSSD and Si(Li) detectors, taking into account proton energy losses in $CD_2$ target and in the dead layers of MUST2 telescopes (see Fig.3 left). Assuming two-body kinematics, excitation energy was calculated by taking into account energy loss in the gas of CATS detectors (see Fig.3 right). An additional selection in time of flight between CATS2 and the plastic was also required to separate contaminants from the beam.

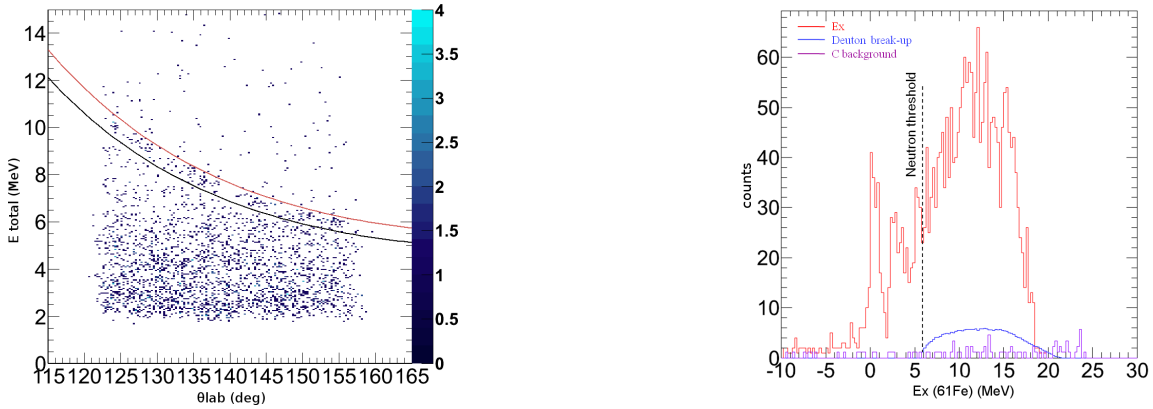


Figure 3: *Left: Experimental kinematic lines energy versus angle for d($^{60}$Fe,pγ)$^{61}$Fe reaction in the laboratory frame; calculated kinematic lines for the 207 keV (in red) and 2160 keV (in black) excited states are plotted for comparison. Right: Excitation energy spectrum of $^{61}$Fe; Carbon background and break-up component are shown.*

Two peaks are observed under the neutron threshold. Based on a full Monte Carlo simulation of the setup and according to DWBA cross-section calculations using spectroscopic factors predicted by shell model calculations [15], three dominant states are expected at 207, 628 keV (experimental data) and at 2160 keV (theoretical prediction). Excited states with spectroscopic factors

lower than 0.01 were not considered. The first peak observed on Fig.3 (right) might be a mixing of the 207 keV and the 628 keV states, whereas the second peak may let appear the 2160 keV state. $\gamma$-ray analysis should allow to improve resolution and to disantangle some of the populated states. The carbon-induced background was evaluated in a dedicated run using a pure carbon target. This component normalized to the number of C nuclei in $CD_2$ target and the number of incident $^{60}$Fe ions is shown Fig.3 (right) in purple. The deuton break-up component (in blue) was evaluated with Monte-Carlo simulations [16] but its normalization still need to be adjusted. However, it will not affect the direct capture part, since it only plays a role above the neutron threshold.

## 4. Conclusion and perspectives

We reported on the first d($^{60}$Fe,p$\gamma$)$^{61}$Fe experiment which was performed at GANIL aiming at studying the $^{60}$Fe(n,$\gamma$)$^{61}$Fe reaction, which plays an important role in $^{60}$Fe nucleosynthesis during s-process in massive stars. Preliminary results for kinematic lines and excitation energies of the populated states of $^{61}$Fe are obtained from charged particle detectors. Peaks are observed below neutron threshold, probably mixing several states of $^{61}$Fe. Hopefully, in the near future, $\gamma$-ray analysis will improve the excitation energy resolution and allow to disantangle some of the populated excited states of $^{61}$Fe. A further theoretical study is needed to evaluated the deuton break-up strength. Angular momentum as well as spectroscopic factors of the different excited states of $^{61}$Fe will be determined by comparison of proton angular distributions with DWBA calculations. This information will then be used to estimate the direct capture component of the cross-section and constrain shell model calculation.

## References

[1] W. Wang et al, *A & A 469, 1005-1012 (2007)*

[2] D. M. Smith, *New Astronomy Reviews 48 (2004) 87-91*

[3] G. Rugel et al, *PRL 103, 072502 (2009)*

[4] S. Mostefaoui et al, *New Astronomy Reviews 48 (2004) 155-159*

[5] K. Knie et al, *PRL 83, 1 (1999)*

[6] S. E. Woosley and T. A. Weaver *1995, ApJS, 101, 181*

[7] M. Lugaro and A. Karakas *New Astronomy Reviews 52 (2008) 416, 418*

[8] E. Uberseder et al, *PRL 102, 151101 (2009)*

[9] E. Runte et al, *NPA 441 (1985) 237-260*

[10] R. Grzywacz et al, *PRL 81, 766-769 (1998)*

[11] R. Anne et al, *NIM B 70, 276 (1992)*

[12] S. Ottini et al, *Nuclear Instr. Methods Phys. Res. A 431 (1999), 476-484*

[13] S. Giron et al, *AIP Conference Proceedings, Volume 1213, pp. 201-204 (2010).*

[14] E. Pollacco et al, *Eur. Phys. J A25, s01, 287-288 (2005)*

[15] G. Martinez-Piñedo, *private communication*

[16] L. Gaudefroy, *PhD thesis*, 2005